

## A METHOD FOR THE DETERMINATION OF THE PLUG INTERFACE AND THE FLOW OF A BINGHAM FLUID BETWEEN ROTATING CYLINDERS

P.F. SIEW<sup>1</sup>, J.A. REIZES<sup>2</sup>, R.R. HORSLEY<sup>1</sup> and S.W. LYE<sup>1</sup>

<sup>1</sup>Curtin University of Technology, GPO Box U1987, Perth, WA 6001, AUSTRALIA

<sup>2</sup>University of New South Wales, Kensington, NSW 2033, AUSTRALIA

### ABSTRACT

In this paper a numerical technique is used to study the flow of a Bingham plastic confined between concentric cylinders with the inner cylinder rotating. The parameters of the problem are chosen so as to produce a plug interface, and the Bingham plastic is modelled as a bi-viscosity fluid. The position of the interface is estimated numerically, as is the flow field in the yielded region. The method of false transients is introduced to accelerate the numerical convergence and the equations are discretised with central differences in both time and space. The resulting system of equations is solved using a judicious mix of SOR and an ADI scheme. Using a projection to zero mesh size, good agreement is obtained between the numerical estimates and the analytic solution for cylinders of infinite length. Numerical results are also presented for finite cylinders with stationary lids.

### INTRODUCTION

This work has its genesis in the study of the flow of clay slurries in a hydrocyclone. It was observed that unless additives are introduced into the flow regime to reduce the effective viscosity there is little or no separation (Horsley and Allen 1987, Horsley et al 1992). The addition of thinning agents tends to change the constitutive properties of the original medium which is a processing technique but tells us very little about the flow field. One possible explanation for the lack of separation in slurries with a significant yield stress may be due to the fact that the spin-up in the hydrocyclone is not sufficiently strong in the cases studied. To date, little is known about the flow field, or whether there is a plug interface. A numerical approach can yield estimates of the position of the interface, but the lack of exact solutions makes it difficult to check the computational accuracy and there are no experimental data since the opaqueness of the slurries makes observation impossible. In an attempt to throw some light on the subject we proceed, as a first step, to consider the flow of a yield pseudo-plastic in a simplified geometry.

It has been observed by several authors (for example Nakamura & Sawada 1987, or Tanner and Milthorpe, 1983) that slurries may be modelled as a Bingham plastic. In such flows, regions in which there is no shear strain rate (the plug) and an adjoining region in which there is a strain rate (yielded region) are often encountered. Flows confined between boundaries of various geometries have been studied by many authors, but analytic solutions for these types of flows are not readily available and recourse has to be made to numerical techniques. In this paper we use a bi-viscosity model to approximate the characteristics of a Bingham plastic confined between finite concentric cylinders with the inner cylinder rotating. The motion is assumed to be axi-symmetric and steady state solutions only are sought. The parameters of the problem have been chosen so as to produce a plug interface. The

method of false transients is introduced to accelerate the numerical convergence and the equations are discretised with central differences in both time and space. Using an ADI scheme, it is found that the convergence rate is, in general, slow and depends critically on the choice of the artificial time constants. However, a judicious mix of SOR and the ADI scheme gives faster convergence in most cases.

The program was run initially with periodic boundary conditions in the axial direction so that solutions for infinite cylinders could be obtained. Good agreement is obtained between the numerical estimates and the analytic solution for this case. The method is then extended to the case of finite cylinders with stationary lids.

### MATHEMATICAL FORMULATION

The constitutive equation for a Bingham plastic linking the deviatoric stress tensor and the rate of strain tensor has been described by Oldroyd (1947) and is represented here by the relationship

$$\begin{aligned} \tau_{ij} &= 2\left[\mu_p + \frac{\tau_0}{\dot{\gamma}}\right]e_{ij}, & \text{for } \frac{1}{2}(\tau : \tau) > \tau_0^2 \\ e_{ij} &= 0, & \text{for } \frac{1}{2}(\tau : \tau) < \tau_0^2 \end{aligned} \quad (1)$$

in which  $\tau_{ij}$  is the stress tensor,  $\mu_p$  is the plastic viscosity,  $\tau_0$  is the yield stress,  $\dot{\gamma} = \sqrt{2e_{ij}e_{ji}}$  is the shear rate,  $e_{ij}$  is the rate of strain tensor, and the scalar product  $\tau : \tau$  is the second invariant of the deviatoric stress tensor. It is noted that the stress tensor is defined only for  $\frac{1}{2}(\tau : \tau) > \tau_0^2$  which means we cannot know what the stress distribution is in the region of the unyielded flow. One assumption taken is that the stress is continuous from the yielded flow region right up to the plug interface.

The equations of motion are valid in the region where the fluid has yielded. However, as observed by Tanner and Milthorpe (1983) it is inconvenient to attempt to distinguish between a state of stress and one of absolute rigidity ( $\dot{\gamma} = 0$ ) and equation (1) cannot be imposed numerically. We therefore find it expedient to adopt the idea expounded by them and replace equation (1) by a bi-viscosity model, viz.

$$\begin{aligned} \tau_{ij} &= 2\left[\mu_p + \frac{\tau_0}{\dot{\gamma}}\right]e_{ij}, & \text{for } \dot{\gamma} \geq \dot{\gamma}_c \\ \tau_{ij} &= 2\left[\mu_p + \frac{\tau_0}{\dot{\gamma}_c}\right]e_{ij}, & \text{for } \dot{\gamma} < \dot{\gamma}_c \end{aligned} \quad (2)$$

where  $\dot{\gamma}_c$  is a predetermined quantity. By keeping  $\dot{\gamma}_c$  small we are effectively replacing the unyielded region by a very viscous fluid.

Although we are interested in the steady state solution, Mallinson and de Vahl Davis (1973) observed that if a unique steady state exists, it may sometimes be obtained more efficiently by introducing fictitious transient



terms into the equations of motion. Cylindrical coordinates  $(r, \theta, z)$  with corresponding velocity vector  $(u, v, w)$  are used to exploit the axial symmetry in the problem, but instead of solving for the primitive variables, the problem may be formulated in terms of the azimuthal component of the vorticity

$$\zeta = \frac{\partial u}{\partial z} - \frac{\partial w}{\partial r},$$

the swirl

$$\Gamma = rv,$$

and the Stokes stream function defined by

$$u = -\frac{1}{r} \frac{\partial \psi}{\partial z}, \quad w = \frac{1}{r} \frac{\partial \psi}{\partial r}.$$

This formulation bypasses the difficulties associated with the imposition of pressure boundary conditions. The method was successfully used by Hughes, et al (1984) in studying Newtonian flow between rotating cylinders. Adopting this method, using  $\Omega^{-1}$  ( $\Omega$  being a convenient angular velocity) as the time scale, and the annular gap between the two cylinders as the length scale  $L$ , the non-dimensional equations of motion are

$$\frac{1}{\alpha_x} \frac{\partial \psi}{\partial t} = \frac{\partial^2 \psi}{\partial r^2} - \frac{1}{r} \frac{\partial \psi}{\partial r} + \frac{\partial^2 \psi}{\partial z^2} + r\zeta, \quad (3)$$

$$\begin{aligned} \frac{1}{\alpha_z} \frac{\partial \zeta}{\partial t} + Re_p \left[ \frac{\partial(ru\zeta)}{\partial r} + \frac{\partial(rw\zeta)}{\partial z} - u\zeta - (1/r^2) \frac{\partial \Gamma^2}{\partial z} \right] \\ = r(\nabla \times (\nabla \cdot \tau))_\theta, \end{aligned} \quad (4)$$

and

$$\begin{aligned} \frac{1}{\alpha_s} \frac{\partial \Gamma}{\partial t} + Re_p \left[ \frac{\partial(ru\Gamma)}{\partial r} + \frac{\partial(rw\Gamma)}{\partial z} \right] \\ = \frac{\partial}{\partial r} [\eta r^3 \frac{\partial}{\partial r} (\Gamma/r^2)] + \frac{\partial}{\partial z} [\eta r^3 \frac{\partial}{\partial z} (\Gamma/r^2)]. \end{aligned} \quad (5)$$

in which  $Re_p = \rho LV/\mu_p$  is the Reynolds number based on the plastic viscosity,  $\rho$  is the density,  $V$  is a typical velocity, and the  $\alpha$ 's are the fictitious time constants. Also in equation (4), the term in brackets on the right hand side can be expressed as

$$\begin{aligned} (\nabla \times (\nabla \cdot \tau))_\theta = \frac{\partial}{\partial r} \left( \frac{\eta}{r} \frac{\partial(r\zeta)}{\partial r} \right) + \frac{\partial}{\partial z} \left( \frac{\eta}{r} \frac{\partial(r\zeta)}{\partial z} \right) \\ - 2 \frac{\partial}{\partial r} (e_{rz} \frac{\partial \eta}{\partial r}) + 2 \frac{\partial}{\partial z} (e_{rr} \frac{\partial \eta}{\partial r}) \\ + 2 \frac{\partial}{\partial z} (e_{rz} \frac{\partial \eta}{\partial z}) - 2 \frac{\partial}{\partial r} (e_{zz} \frac{\partial \eta}{\partial z}), \end{aligned}$$

and

$$\eta = \left[ 1 + \frac{W_e}{\dot{\gamma}} \right],$$

in which  $W_e = \tau_o L/(\mu_p V)$  is the Weissenberg number.

The above equations are replaced by a central difference scheme by imposing a mesh over the flow region. The resulting set of linear equations is solved using a method due to A.A. Samarskii and V.B. Andreev, as described in Mallinson and de Vahl Davis (1973). As is shown below, great care has to be taken in interpreting the results of the computation and a double projection has to be done to obtain the velocity profile.

## BOUNDARY CONDITIONS

If  $l$  denotes the length of the two cylinders with internal and external radii  $R_i$  and  $R_o$  respectively, the boundary conditions on the stream function are the same

whether  $l$  is finite or infinite. For the finite case, we assume  $\psi$  is zero on all boundaries. In the infinite case the assumption that a steady state exists means that the only non-zero component of velocity is in the azimuthal direction which means that  $\psi$  is identically zero everywhere. If  $\Omega_i$  and  $\Omega_o$  denote the angular velocities of the inner and outer cylinder respectively then

$$\Gamma(R_i, \theta, z) = R_i^2 \Omega_i, \quad \Gamma(R_o, \theta, z) = R_o^2 \Omega_o, \quad (6)$$

and assuming no slip, the boundary conditions at the ends are given by

$$\Gamma(r, \theta, \pm l/2) = 0. \quad (7)$$

The boundary condition on the vorticity field is obtained by expanding in a Taylor series giving

$$\zeta_b = \frac{24(\psi_b - \psi_1)}{h^2(8r_b + 5h)} - \frac{(4r_b + 3h)\zeta_1}{8r_b + 5h} \quad (8)$$

where subscript  $b$  denotes the value of the quantity on the boundary while subscript  $1$  denotes the value of the quantity a distance  $h$  from the boundary in the flow region. In the numerical scheme below,  $h$  is the mesh size used for the discretization.

When  $l$  is infinite, periodic conditions on  $\Gamma$  and  $\zeta$  are used [see for example, Dinar and Keller (1988)].

## CYLINDERS WITH INFINITE ASPECT RATIOS

The aspect ratio  $A_r$  is the ratio of the length of the cylinders to the annular gap. When  $A_r$  is infinite, analytic solutions are obtainable and it is possible to check the accuracy of the numerical procedure. It is convenient to set one of the cylinders at rest while rotating the other one. The position of the interface is unaffected so long as the angular velocity has the same magnitude. In our implementation therefore, we arbitrarily set  $\Omega_o$  to zero.

The analytic solution for an ideal Bingham fluid is well known and its velocity distribution is given in dimensionless form by

$$v_b = r W_e \left[ \log(r/r_o) - \frac{1}{2}(1 - r_o^2/r^2) \right], \quad R_i \leq r \leq r_o, \quad (9)$$

in which  $r_o$  is the plug radius. On the inner cylinder equation (9) yields

$$\Omega_i = W_e \left[ \log(R_i/r_o) - \frac{1}{2}(1 - r_o^2/R_i^2) \right]. \quad (10)$$

For a given choice of  $W_e$  the true plug radius can be calculated from equation (10). Now, using the same solution method the equations for the biviscosity model can also be solved giving

$$\begin{aligned} \frac{v}{r} = \frac{v_b}{r} + \frac{W_e}{2} \left( \frac{1}{R_i^2} - \frac{1}{r^2} \right) \left[ r_o^2 - \left( 1 + \frac{\dot{\gamma}_c}{W_e} \right) r_c^2 \right], \quad \dot{\gamma} > \dot{\gamma}_c \\ = \frac{\dot{\gamma}_c r_c^2}{2} \left( \frac{1}{r^2} - \frac{1}{R_o^2} \right), \quad \dot{\gamma} < \dot{\gamma}_c \end{aligned} \quad (11)$$

in which  $r_c$  is the radius at which  $\dot{\gamma} = \dot{\gamma}_c$ . When  $\dot{\gamma}_c = 0$  the first of equation (11) becomes equation (9), otherwise equation (11) always gives higher velocity values than equation (9). The discrepancy vanishes as  $\dot{\gamma}_c$  approaches zero. Equating velocities at  $r = r_c$  yields the relation

$$\dot{\gamma}_c = \frac{2W_e R_i^2 R_o^2}{r_c^2 (R_o^2 - R_i^2)} \left[ \frac{1}{2} \left( 1 - \frac{r_c^2}{R_i^2} \right) + \log \left( \frac{r_c}{R_i} \right) + \frac{\Omega_i}{W_e} \right], \quad (12)$$



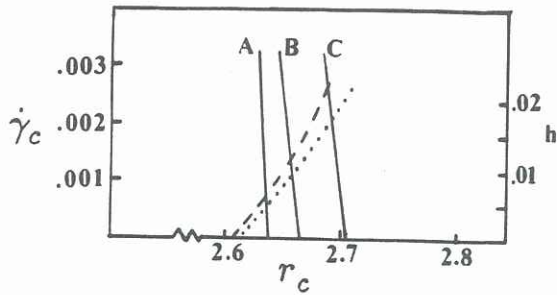


Fig. 1 Plot of  $\dot{\gamma}_c$  against  $r_c$  for three different mesh sizes: A ( $h = .005$ ), B ( $h = 0.01$ ) and C ( $h = 0.02$ ). The projections to zero mesh is shown by the dotted line for  $r_c$  and the dashed line for  $r_t$ .

which is useful for checking purposes. Another useful quantity is the non-dimensional stress, scaled by  $\tau_0$  so that it is unity on the plug interface, given by

$$\tau = \frac{r_c^2}{r^2} \left( 1 + \frac{\dot{\gamma}_c}{W_e} \right). \quad (13)$$

If  $r = r_t$  when  $\tau = 1$ , we may use  $r_t$  as another estimate for the plug radius.

In the numerical procedure, we set  $W_e = 6.05$ ,  $\Omega = 0.5$  and  $Re_p = 53.2$ . The radii of the cylinders are set at 0.1 and 0.15 metres so that  $L = 0.05$  and the dimensionless values are  $R_i = 2$  and  $R_o = 3$  and using equation (10), this gives a plug radius of 2.6. Using (12), it is easy to show that  $d\dot{\gamma}_c/dr_c < 0$  and that  $\dot{\gamma}_c = 0$  at  $r_c = 2.6$ . Using equations (3) to (5) the numerical procedure actually overestimates the value of  $r_c$  so that given a  $\dot{\gamma}_c$  the value of  $r_c$  is equal to  $r_o + \epsilon$  for some small  $\epsilon > 0$ . This means that numerically,  $r_c$  will give an over-estimation for the true plug radius and this gets worse as  $\dot{\gamma}_c$  approaches zero. However the error is uniformly less as the mesh size is reduced. Figure 1 gives a plot of  $\dot{\gamma}_c$  against  $r_c$ .  $h$  is taken as 0.02, 0.01 and 0.005 and in each case  $\dot{\gamma}_c$  takes on the values 0.003, 0.002 and 0.001. The limiting values of  $r_c$  as  $\dot{\gamma}_c \rightarrow 0$  for each mesh size are used to project to zero mesh size, giving the estimated plug radius as 2.615 which is accurate to within 1%. This is given by the dotted line in the figure. On the other hand as  $\dot{\gamma}_c$  changes over the above range, for each mesh size,  $r_t$  remains unchanged to 4 significant digits, and in each case is nearer to the true plug radius although it is still an overestimation. Projecting the value of  $r_t$  to zero mesh gives the estimated plug radius as 2.61. The result is also shown in Figure 1. It is clear from the figure that  $r_t$  gives a much better indication of the position of the plug interface.

The numerical procedure underestimates velocities consistently and lowering  $\dot{\gamma}_c$  increases the divergence from the correct values. In fact, by differentiating the first of equation (11) we can show that  $dv/d\dot{\gamma}_c > 0$ , which is in agreement with the above result. However, reducing the mesh size brings the velocity uniformly nearer to that predicted by equation (9) which again suggests that a double projection is required. For each mesh size, the limiting value of the velocity is obtained by projecting  $\dot{\gamma}_c$  to zero. Since the velocity  $v_b$  for the ideal Bingham fluid is known, an analysis of the numerical errors for each mesh size may be made. The results suggests an error of  $O(h^{1.7})$  near the inner cylinder increasing to about  $O(h^{1.5})$  near  $r = r_c$ . The error of the procedure therefore appears to be better than linear. The limiting velocity obtained for the three different mesh sizes are projected to zero mesh size using a Richardson extrapolation scheme of second order and the resulting velocity  $v_l$  is compared with  $v_b$  in Table I below. The above method gives close to three significant figure accuracy for the yielded flow near the inner cylinder. The accuracy

reduces as the plug radius is approached which is what we expect since the biviscosity model will always have velocity decaying to zero only at the outer cylinder. An important observation is the fact that, numerically the bi-viscosity model cannot give accurate velocities if one chooses a fixed  $\dot{\gamma}_c$ , however fortuitous the choice may be. Tanner and Milthorpe (1983) attempted to find an "optimal" constant value of  $\dot{\gamma}_c$  by numerical experimentation. There is no optimal value in the case discussed here as a large value of  $\dot{\gamma}_c$  appears to give "better" values of velocities, but not  $r_c$ , so that the double projection method appears to be the only one at present available which ensures accurate results. Further the limitations of computer performance which may have encouraged Tanner and Milthorpe to use a constant  $\dot{\gamma}_c$  are being quickly removed, so that whilst the method proposed in this paper is expensive, it is not inordinately so and should be used in research.

Table I. Velocity profiles

$r$	$v_b$	$v_l$	$r$	$v_b$	$v_l$
2.0	1.0000	1.0000	2.6	0	0.0002
2.1	0.6717	0.6715	2.7		0.0001
2.2	0.4165	0.4159	2.8		0.0001
2.3	0.2273	0.2265	2.9		0.0000
2.4	0.0982	0.0972	3.0		0
2.5	0.0239	0.0235			

## CYLINDERS WITH FINITE ASPECT RATIOS

The same parameter values are taken as for the previous section but now equations (7) and (8) are applied on the top and bottom lids. Assuming axial symmetry, the flow depends on  $r$  and  $z$  only. One disadvantage here is the fact that there are no theoretical results with which to make comparisons. However when the aspect ratio is large, we expect that the azimuthal velocity profile along the centreline of the cylinders will be close to that for the case of infinite aspect ratio. In fact, when  $A_r = 6$  the velocity profile along the centreline agrees with that of  $v_l$  in Table I to two decimal places.

We now use a slightly different method to estimate the location of the plug interface. The method is suggested by the steadiness in the value of  $r_t$  as noted in the previous section. In all the runs made, the value of  $r_t$  along the centreline of the cylinders changes very slowly and is constant to 4 significant digits for each mesh size provided  $\dot{\gamma}_c$  is small enough. This is true for  $\dot{\gamma}_c < .003$ . It is therefore sufficient to make one run at each mesh size and record the value of  $r_t$ . These values are then projected to zero mesh size to give the position of the plug interface. Figure 2 gives the estimated plug radii along the centreline of the cylinders for three different aspect ratios. Decreasing the aspect ratio draws the plug interface closer towards the inner rotating cylinder.

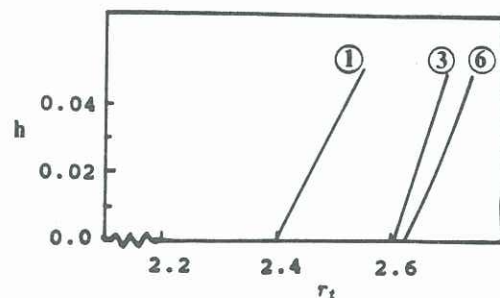


Fig. 2 Plot of the mesh size  $h$  against  $r_t$  along the centreline of the cylinders for aspect ratios 1, 3 and 6 as labelled.



In fact, the projection to zero mesh size can be done along the entire length of the cylinders giving the estimated plug interface shown in Figures 3 and 4. We note that the method is inappropriate if we want to obtain the velocity fields since a double projection would be required as in the previous section.

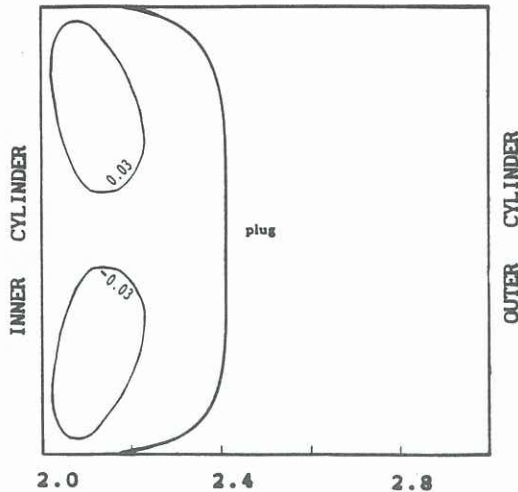


Fig. 3 The stream function map for  $A_r = 1$ . The estimated plug interface is the right boundary curve.

The axial and radial velocities are best shown by looking at the stream function maps. To obtain good estimates of the stream function values, we suspect that a double projection as was done for the azimuthal velocity field in the previous section would be required. This is

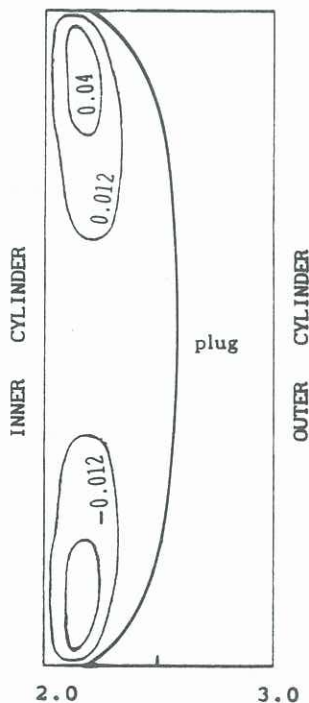


Fig. 4 The stream function map for  $A_r = 3$ . The estimated plug interface is the right boundary curve.

ongoing work and will not be reported here. Instead, we note that a good qualitative picture of the flow field can be gleaned from the contours obtained for a low value of  $\hat{\gamma}_c$ . This is shown in Figures 3 and 4 for aspect ratios of 1 and 3 respectively. In each case, there appears to be two weak cells as expected.

## DISCUSSION

Whether the aspect ratio is finite or infinite, the rate of numerical convergence is highly sensitive to the choice of values for the set of artificial time constants  $\Xi = \{\alpha_x, \alpha_s, \alpha_z\}$  in equations (3) to (5). Typically, a 'wrong' choice of values for this set may cause the iterations to diverge. When it looks as if convergence might occur, the rate is very slow. For a suitable set of values for  $\Xi$ , the iteration may slowly appear to converge for a while and then start to diverge. One option is to save all parameters and stop the process at this turnaround stage, effect a change to the set of values and continue the iteration. We have found that replacing the solution for one of the field variables by an SOR scheme gives faster convergence and this was exploited where possible. For the finite cylinders, it is faster still if, when the iterations appear to be slowly converging, the vorticity and stream function fields are calculated by SOR schemes. Depending on the mesh size, between 3000 to 5000 iterations are required for each point on the  $\hat{\gamma}_c - r_c$  curve of Figure 1.

As mentioned earlier, this is an ongoing project and one way to obtain more accurate estimate for the flow field for finite cylinders is to map the yielded region onto a square say thereby allowing the field parameter to be calculated at a sufficient number of points to make the contour plot more accurate. A logical extension to this project is to study the onset of multiple solutions by increasing the rotation speed.

## ACKNOWLEDGEMENTS

We are grateful to Dr E Leonardi of the School of Mechanical and Industrial Engineering at the University of New South Wales, whose computer program for Newtonian flow was adapted to cater for this non-Newtonian project.

## REFERENCES

- Dinar, N and Keller, H B (1988) Computations of Taylor vortex flows using multigrid continuation methods. In *Recent advances in computational fluid dynamics*, C C Chao, S A Orszag and W Shyy, ed., Springer-Verlag, New York, 43, 191-262.
- Horsley, R R, and Allen, D W (1987) The effect of yield stress on hydrocyclone performance in the mining industry. *Proc. 3rd Int. Conf. Hydrocyclones*, Oxford, (BHRA) 269-275.
- Horsley, R R, Tran Q K, and Reizes, J A (1992) The effect of rheology on the performance of hydrocyclones. *Proc. 4th Int. Conf. Hydrocyclones*, Southampton, (BHRA), to appear.
- Hughes, C T, Leonardi, E, de Vahl Davis, G, and Reizes, J A (1985) A numerical study of the multiplicity of flows in the Taylor experiment. *Physico-Chemical Hydrodynamics*, 6, 637-645.
- Mallinson, G D and de Vahl Davis, G (1973) The method of the false transient for the solution of coupled elliptic equations. *J. Comp. Phys.*, 12, 435-461.
- Nakamura, M and Sawada, T (1987) Numerical study on the laminar pulsatile flow of slurries. *J Non-Newtonian Fluid Mech.*, 22, 191-206.
- Oldroyd, J G (1947) A rational formulation of the equations of plastic flow for a Bingham fluid. *Proc Camb Phil Soc*, 43, 100-105.
- Tanner, R I and Milthorpe, J F (1983) Numerical simulation of the flow of fluids with yield stresses. *Proc. 3rd Int. Conf. Numerical Methods in Laminar and Turbulent Flow*, C Taylor, J A Johnson, and W R Smith, ed., 680-690.